

This article was downloaded by:

On: 25 January 2011

Access details: *Access Details: Free Access*

Publisher *Taylor & Francis*

Informa Ltd Registered in England and Wales Registered Number: 1072954 Registered office: Mortimer House, 37-41 Mortimer Street, London W1T 3JH, UK



## Liquid Crystals

Publication details, including instructions for authors and subscription information:

<http://www.informaworld.com/smpp/title~content=t713926090>

### The influence of charge-transfer interactions on solid and cholesteric liquid crystalline mixtures of cholesteryl anthraquinone-2-carboxylate and cholesteryl 9,10-dimethoxyanthracene-2-carboxylate

Emanuele Ostuni; Richard G. Weiss

Online publication date: 06 August 2010

**To cite this Article** Ostuni, Emanuele and Weiss, Richard G.(1999) 'The influence of charge-transfer interactions on solid and cholesteric liquid crystalline mixtures of cholesteryl anthraquinone-2-carboxylate and cholesteryl 9,10-dimethoxyanthracene-2-carboxylate', *Liquid Crystals*, 26: 4, 541 – 551

**To link to this Article:** DOI: 10.1080/026782999204985

**URL:** <http://dx.doi.org/10.1080/026782999204985>

PLEASE SCROLL DOWN FOR ARTICLE

Full terms and conditions of use: <http://www.informaworld.com/terms-and-conditions-of-access.pdf>

This article may be used for research, teaching and private study purposes. Any substantial or systematic reproduction, re-distribution, re-selling, loan or sub-licensing, systematic supply or distribution in any form to anyone is expressly forbidden.

The publisher does not give any warranty express or implied or make any representation that the contents will be complete or accurate or up to date. The accuracy of any instructions, formulae and drug doses should be independently verified with primary sources. The publisher shall not be liable for any loss, actions, claims, proceedings, demand or costs or damages whatsoever or howsoever caused arising directly or indirectly in connection with or arising out of the use of this material.

# The influence of charge-transfer interactions on solid and cholesteric liquid crystalline mixtures of cholesteryl anthraquinone-2-carboxylate and cholesteryl 9,10-dimethoxyanthracene-2-carboxylate

EMANUELE OSTUNI and RICHARD G. WEISS\*

Department of Chemistry, Georgetown University, Washington, DC 20057-1227, USA

(Received 20 September 1998; accepted 13 October 1998)

The phase behaviour of 3 $\beta$ -cholesteryl 9,10-anthraquinone-2-carboxylate (CAQ, an excellent electron acceptor) and 3 $\beta$ -cholesteryl 9,10-dimethoxyanthracene-2-carboxylate (CMAQ, an excellent electron donor) have been investigated neat and as mixtures by a variety of techniques. Both molecules form thermotropic cholesteric phases. UV-Vis absorption spectra of CAQ:CMAQ mixtures provide strong evidence for the formation of charge-transfer (CT) complexes in the solid state. DSC thermograms of the mixtures reveal several transitions, only some of which are observable by optical microscopy. The mesophase range of CAQ is increased by *c.* 40° upon addition of as little as 10 wt% of CMAQ as a consequence of increased attractive forces in the CT complexes. X-ray powder diffraction patterns confirm that CAQ forms different crystalline phases upon being cooled from the mesophase and by recrystallization from solvents. The 5:5 mixture can be supercooled to a glass from its cholesteric phase. Some of the phase behaviour of the CAQ:CMAQ mixtures is explained with a model that includes selective crystallization of the two components into eutectics from supercooled liquid crystalline matrices.

## 1. Introduction

The intermolecular interactions responsible for formation of thermotropic mesophases by binary mixtures of non-mesogenic molecules or the stabilization of a mesophase by a non-mesogenic moiety [1, 2] are of considerable interest; the intermolecular interactions that are responsible for such phenomena are the subject of much investigation [3]. In an extensive review, Gray noted that liquid crystalline phases from binary mixtures seem to occur through a delicate balance of thermodynamic parameters affecting the depression of transition temperatures of the neat components [4]. Dave and Dewar found that the temperature range of the mesophase of *p*-azoxyanisole can be increased by non-mesogenic *p*-azo- and *p*-azoxy-benzenes, and the magnitude of the increase is greater the more polar the substituent [2]. More recently, Sheikh-Ali and Weiss observed nematic phases in binary mixtures of non-mesogenic 4-alkyl-*N*-(4-cyanophenyl)piperidines [1]. The clearing temperatures of mixtures were depressed to the largest extent at the eutectic compositions and increased for longer alkyl groups.

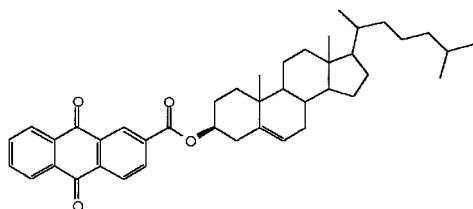
Charge-transfer (CT) interactions have been used extensively to induce and increase the range of discotic mesophases comprising low molecular mass molecules with stiff aromatic cores and flexible aliphatic side chains [5]. An aromatic donor or acceptor molecule without aliphatic chains can intercalate in the discotic columns. CT interactions within the columns make close packing of aliphatic chains even more difficult and result in a net higher mobility of the molecular system and a lower flow viscosity [6].

Very few examples of CT-stabilization in mesophases of rod-like molecules are known. Kosaka and Uryu found that a rod-like electron acceptor stabilizes the nematic phase of a rod-like electron donor and induces a smectic phase [7]. Although CT interactions were suggested as the major contributor to the stabilization of the mesophase, spectroscopic evidence was not provided, and formation of a eutectic mixture was postulated at compositions in which the induced smectic phase was observed. Recently, CT interactions have been used to stabilize smectic A phases [8] in thermotropic liquid crystals (LCs) and to induce cholesteric phases in nematic lyotropic mixtures [9].

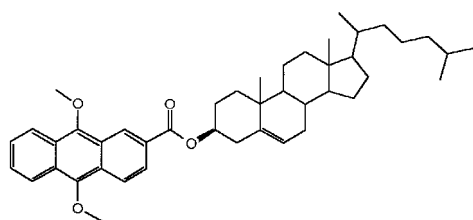
Here, we describe the consequences of mixing the mesogenic and structurally similar molecules, 3 $\beta$ -cholesteryl

\* Author for correspondence.

9,10-dimethoxyanthracene-2-carboxylate (CMAQ) and 3 $\beta$ -cholesteryl 9,10-anthraquinone-2-carboxylate (CAQ) [10, 11]. Charge-transfer interactions between the electron-poor anthraquinone [12] and electron-rich 9,10-dimethoxyanthracene [13] groups (both of which are quite polarizable [14–16]) lead to stabilized cholesteric phases whose properties are very different from those of either neat component.



CAQ



CMAQ

## 2. Experimental

### 2.1. Instrumentation

Ultraviolet-visible (UV-Vis) absorption spectra were recorded on a Perkin-Elmer Lambda 6 spectrophotometer interfaced to a PC. Solid samples were sandwiched between two quartz plates with a teflon spacer.

Differential scanning calorimetry (DSC) thermograms were recorded with a Du Pont 910 differential scanning calorimetry cell base interfaced to a TA 2000 Thermal Analyst. All samples were heated at 10° min<sup>-1</sup> from 30° to 210°C and cooled at 2° min<sup>-1</sup> (using a steady nitrogen flow) after a one minute isothermal period. Overlapping peaks were analysed with the manufacturer's software package by dividing them at the point where they cross with a line drawn to the baseline. All numerical analyses are based on at least two data sets from consecutive, reproducible heating/cooling cycles. Infrared spectra were recorded on a Midac FT-IR spectrometer using KBr pellets.

Optical microscopy (OM) studies were performed using a Leitz 585 SM LUX POL microscope equipped with linear polarizers, a Pentax 35 mm camera, and a Leitz 350 heating stage. Samples were sandwiched between two glass slides. Phase transition temperatures reported in this section were measured with the microscope and a calibrated Omega HH21 microprocessor thermometer connected to the hot stage by a J-K-T thermocouple. Liquid crystalline textures were assigned following Demus and Richter [17].

Nuclear magnetic resonance (NMR) spectra were recorded on a Bruker AM-300 spectrometer equipped with a Bruker 5 mm probe and interfaced to an Aspect 3000 computer or on a Nicolet 270 MHz spectrometer interfaced to a MacIntosh Quadra 900 computer.

High performance liquid chromatography (HPLC) was performed with a Waters 6000A solvent delivery system at 2 ml min<sup>-1</sup>, a Waters U6K injector, and an Alltech Econosphere Silica 5U column (25 cm × 4.6 mm i.d.) attached to a Model 450 detector ( $\lambda = 254$  nm). Peaks were integrated either by cutting and weighing or by hand integration with the aid of a K + E Paragon compensating polar planimeter.

X-ray powder diffraction patterns were recorded on an Inel CPS 120 diffractometer with a XRG 3000 X-ray generator using Cu K $\alpha$  ( $\lambda = 1.542$  Å) radiation; temperature was controlled with a Minco CT 137 temperature controller connected to a custom made oven†. The samples were placed in capillaries (i.d. 1.5 mm) of completely randomized glass (Charles Supper Co.) that were mounted with glue. Chemical ionization (NH<sub>3</sub>) mass spectral data were obtained on a Finnigan 4600 spectrometer by Dr. Quanlong Pu at the National Institutes of Health, Bethesda, Maryland, USA.

Samples of CAQ and CMAQ (expressed as weight:weight ratios) were prepared by evaporating methylene chloride solutions under vacuum. Since CAQ and CMAQ have very similar molecular masses (620 and 650 g mol<sup>-1</sup>, respectively), their weight and molar ratios are almost the same.

### 2.2. Materials

All chemicals were used as received unless noted otherwise. Infrared and <sup>1</sup>H NMR spectra of the three molecules whose syntheses are described below are included as *Supplementary Material*\*.

#### 2.2.1. 9,10-Dimethoxyanthracene-2-carboxylic acid (DIMAC) [18]

A mixture of 5.04 g (0.02 mol) anthraquinone-2-carboxylic acid (TCI), 40 ml 20% aqueous NaOH and 8 ml ethanol was stirred and heated to 100°C under a dry N<sub>2</sub> atmosphere. The white suspension immediately acquired a deep red colour and became warm after the addition of 2.00 g (0.03 g-atom) of freshly ground zinc. After returning to room temperature, the mixture was heated to *c.* 90°C as 22.5 ml of methyl *p*-toluenesulfonate

† XRD patterns were recorded in the laboratory of Professor Timothy M. Swager with the help of Mr. Bing Xu at the University of Pennsylvania, Philadelphia, Pennsylvania, USA.

\*The *Supplementary Material* data is available from the British Library Document Supply Centre, Boston Spa, Wetherby, Yorkshire LS23 7BQ, UK (publication number 90483). For further details refer to any published issue of the Journal.

were added dropwise. The reaction mixture was cooled to room temperature after the red colour disappeared. The mixture was then combined with *c.* 300 ml of a saturated basic aqueous solution of sodium dithionite, stirred, and filtered. The resulting lobster-coloured precipitate was stirred with 300 ml of *c.* 18% HCl to give a bright yellow precipitate which, after recrystallization from hot ethanol, provided 3.93 g (70% yield) of crystals, m.p. 192–219°C (decomp). <sup>1</sup>H NMR (300 MHz, CDCl<sub>3</sub>, TMS): δ 9.2–7.5 (7 H, m, aryl), 4.2–4.1 (6 H, 2 singlets, methoxy groups), 1.6 ppm (s, moisture). IR (KBr): 3441, 1700, 1620, 1564 cm<sup>-1</sup>.

### 2.2.2. 3β-Cholesteryl 9,10-dimethoxyanthracene-2-carboxylate (CMAQ) [19, 20]

The reaction and work-up were conducted in the dark or under dim light. A mixture of 1.41 g (5.0 mmol) DIMAC, 3.6 ml (50 mmol) dry thionyl chloride, and 500 ml dry benzene was heated under reflux in a dry atmosphere for 12 h. Benzene and thionyl chloride were removed by distillation at atmospheric pressure, and the solid residue was twice dissolved in 250 ml of dry benzene and reduced to residue. The solid was mixed with 0.125 g (5.14 g-atom) magnesium, 1.93 g (5.0 mmol) cholesterol (Kodak) and a few iodine crystals in 200 ml of dry benzene. After 36 h reflux under a dry atmosphere, the mixture was washed with mildly basic water and extracted with chloroform. The organic layer was then washed with a saturated solution of sodium bicarbonate, dried with sodium sulphate, and filtered. The solvent was removed at aspirator pressure. The solid yellow residue was flash-chromatographed several times on a neutral silica column (eluant: toluene) and recrystallized twice in the dark from hot ethyl acetate to yield 1.76 g (54% yield) of bright yellow crystals (*T*<sub>Cr→LC</sub> 173°C; *T*<sub>LC→I</sub> 190°C), 99% pure by HPLC (eluant: 97:3 hexane:ethyl acetate). <sup>1</sup>H NMR (270 MHz, CDCl<sub>3</sub>, TMS): δ 9.2–7.4 (7 H, m, aryl), 5.5 (1 H, d, cholesteryl alkenyl), 5.0 (1 H, m, cholesteryl C3), 4.2–4.1 (6 H, 2 singlets, methoxy groups), 2.56–0.7 ppm (43 H, m, cholesteryl). IR (KBr): 1713 (ester carbonyl), 1624 cm<sup>-1</sup>. CI MS: *m/z* 668 (M+1+NH<sub>3</sub>), 651 (M+1), 386 (M-264, cholesterol), 369 (M-281, dehydrocholesterol).

### 2.2.3. 3β-Cholesteryl anthraquinone-2-carboxylate (CAQ) [19, 20]

The reaction and work-up were conducted in the dark or under dim light. A solution of 1.20 g (4.8 mmol) anthraquinone-2-carboxylic acid (TCI), 3.5 ml (48 mmol) dry thionyl chloride, and 100 ml dry benzene was heated under reflux in a dry atmosphere for 1.75 h and then cooled to 40–50°C. Benzene and thionyl chloride were removed by distillation at atmospheric pressure, and the solid residue was twice dissolved in 100 ml of dry benzene

and reduced to solid. The solid was mixed with 0.117 g (4.8 g-atom) magnesium, 1.84 g (4.8 mmol) cholesterol (Kodak) and a few iodine crystals in 80 ml of dry benzene. After 36 h reflux under a dry atmosphere, the mixture was washed with mildly basic water and extracted with chloroform. The organic layer was then washed with a saturated solution of sodium bicarbonate, dried with sodium sulphate, and filtered. The solvent was removed under aspirator pressure and the resulting yellow solid flash-chromatographed on a neutral silica column with toluene as the eluant. The crude product was dissolved in a minimal amount of chloroform and triturated at room temperature with methanol to yield 0.76 g (26% yield) of yellow crystals (*T*<sub>Cr→LC</sub> 159°C; *T*<sub>LC→I</sub> 228°C; lit. [19] *T*<sub>Cr→LC</sub> 170°C; *T*<sub>LC→I</sub> 229°C), 99% pure by HPLC using the same system described for CMAQ. <sup>1</sup>H NMR (270 MHz, CDCl<sub>3</sub>, TMS): δ 9.0–7.8 (7 H, m, aryl), 5.5 (1 H, d, cholesteryl alkenyl), 5.0 (1 H, m, cholesteryl C3), 2.6–0.7 ppm (43 H, m, cholesteryl). IR (KBr): 1733 (ester carbonyl), 1678 (quinone carbonyl), 1597 cm<sup>-1</sup>. CI MS: *m/z* 638 (M+1+NH<sub>3</sub>), 386 (M-238, cholesterol), 368 (M-256, dehydrocholesterol).

## 3. Results

### 3.1. Charge-transfer complex formation between CAQ and CMAQ

In other work [10, 11, 19, 21], we have found that low concentrations of CAQ can gel 1-octanol or hexadecane (among other liquids). The addition of small amounts of CMAQ to CAQ leads to orange-coloured gels that are thixotropic in some cases [10, 11]. Both solids are yellow when separated.

To determine the origin of the colour change, the absorption spectra of CAQ:CMAQ mixtures were recorded under a variety of conditions. The spectrum of a saturated tetrahydrofuran (THF) solution containing 0.012 M each of CAQ and CMAQ shows only features present in the spectra of the isolated components, figure 1(a).

Evaporation of a 1:1 (mol:mol) THF solution of CAQ and CMAQ on a quartz plate left an orange solid whose UV-Vis absorption spectrum is shown in figure 1(b). Subtracting spectra of solid CAQ and CMAQ, corrected for scattering, from the 1:1 solid according to equation (1) (where  $A_{x+y}(\lambda)$ ,  $A_x(\lambda)$ , and  $A_y(\lambda)$  are the spectra of the 1:1 mixture and the two components, respectively, in their solid phases;  $\alpha$ ,  $\beta$ , and  $C$  are empirically determined constants) leaves a band centered at *c.* 500 nm that is devoid of contributions from the single components, figure 1(b). *This band is compelling evidence for a CT complex between CAQ and CMAQ in the solid state.* A similar band was also obtained from the spectrum of solid 8:2 CAQ:CMAQ.

$$\Delta A_{\lambda} = A_{x+y}(\lambda) - \alpha A_x(\lambda) - \beta A_y(\lambda) - C \quad (1)$$

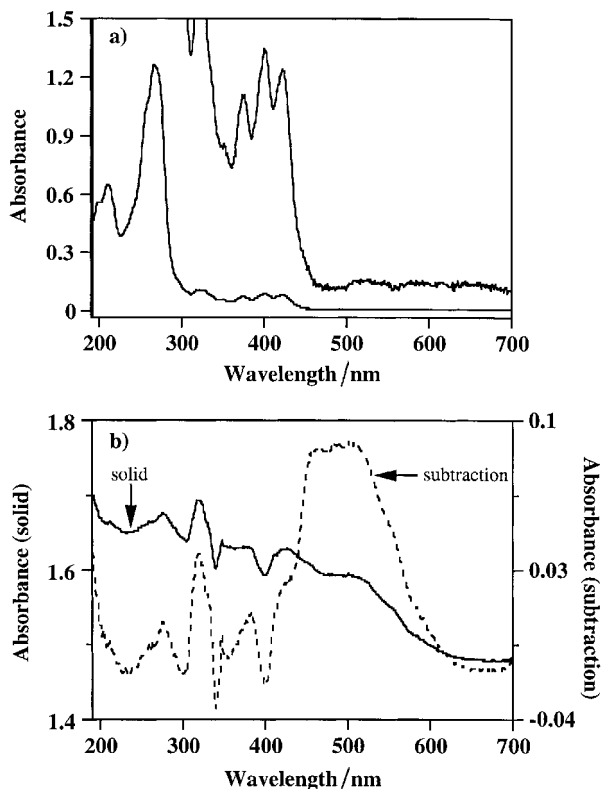


Figure 1. UV-Vis absorption spectra of CAQ:CMAQ mixtures. (a) THF solution of 0.012M CAQ and 0.012M CMAQ showing the long wavelength region in an expanded scale; path length = 100  $\mu\text{m}$ . (b) (—) Solid film deposited on a quartz plate by evaporation of a 1:1 (mol:mol) solution and sandwiched between quartz plates (path length = 0.024 mm). (...) Subtraction of spectra from neat solid CAQ and neat solid CMAQ from the 1:1 solid spectrum according to equation (1).

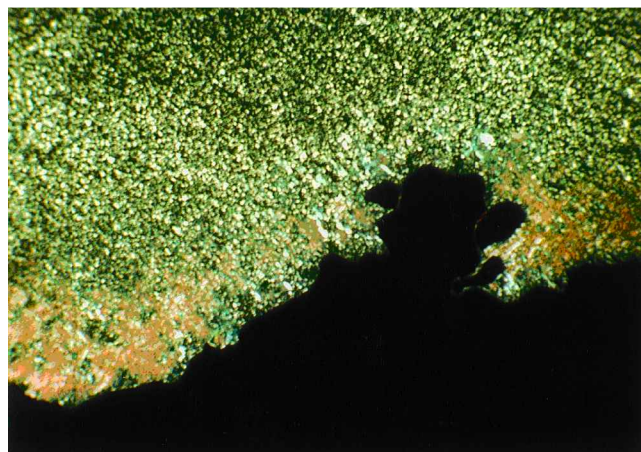
### 3.2. Optical microscopy

Upon heating CAQ, a cholesteric texture with oily streaks [17] appeared at 159°C and cleared at 228°C. A platelet texture, reminiscent of a blue cholesteric phase, was observed over a range of 1–2° upon cooling isotropic CAQ to just below the clearing temperature. It may arise from transient scattering of light from shrinking pre-organized domains; although isotropic scattering between parallel polarizers was not observed, contrary to expectations for a blue phase [17], the presence of one cannot be eliminated. Upon further cooling, a highly birefringent focal conic texture developed that is typical of unperturbed cholesterics with domains whose helical axes are aligned perpendicular to the direction of viewing [22]. Applying pressure to the sample led to the previously detected schlieren texture with oily streaks (indicative of domains with helical axes aligned parallel to the direction of viewing [22]). This pattern remained down to room temperature due to super cooling of the

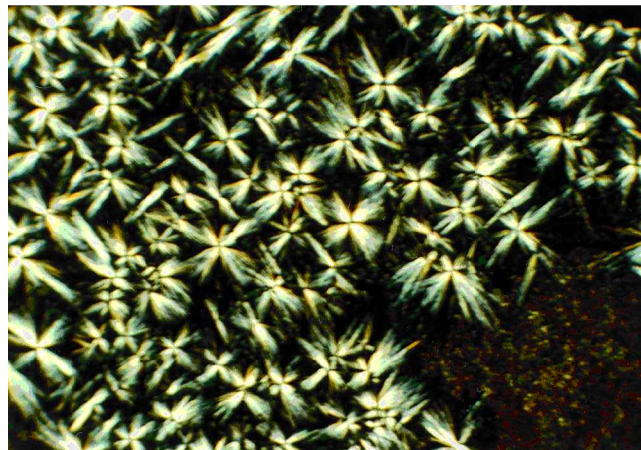
sample. The optical patterns of CMAQ are similar to those of CAQ; the cholesteric range is 173–190°C.

Only optical microscopic patterns of the LC phases of mixtures of CAQ and CMAQ subsequent to initial heating were quantitatively reproducible because proper mixing occurs only at temperatures above  $T_{\text{Cr} \rightarrow \text{LC}}$ . However, all mixtures examined were orange and birefringent at room temperature. During their first heating and cooling, the optical textures were the same as those of neat CAQ and CMAQ, but the transition temperatures were composition dependent. Crystallizations of cooled samples were difficult to observe.

During second heating of CAQ:CMAQ mixtures with 10–40 wt % CAQ, no sharp transitions were detected prior to clearing. When reheated to >88°C, the 8:2 mixture (a glassy cholesteric texture at room temperature) became a viscous liquid with an optical birefringent texture typical of a smectic C phase, figure 2(a) [17];



(a)



(b)

Figure 2. Optical micrographs of CAQ:CMAQ mixtures between crossed polarizers (340X): (a) 8:2, second heating at 105°C; (b) 6:4, second heating at 122°C.

pressure on the cover slips did not deform the texture. At 145°C pressure on the cover slips led to an oily streak (cholesteric) texture. A similar transition, to an apparent smectic C phase, was observed at 91°C upon second heating of the 7:3 mixture; at 150°C, the birefringence increased and the schlieren texture of a cholesteric phase was observed when pressure was applied. Crystallization was evident at 124°C [figure 2(b)] during second heating of the 6:4 and 5:5 mixtures, and cholesteric oily streak patterns could be induced at 155 and 157°C, respectively.

The stability of the mesophase mixtures can be assessed qualitatively from  $T_{LC \rightarrow I}$  during first heating since samples should be homogenized at these temperatures. Minor decomposition, occurring at high temperatures, affects the clearing temperatures of subsequent heating cycles. As a compromise, cholesteric temperature ranges from first heating of the mixtures are reported in table 1. Samples were heated and cooled at approximately the same rates in an attempt to normalize decomposition. *All mixtures clear at temperatures considerably higher than those of neat CAQ or CMAQ, and their mesogenic ranges are greater by factors of c.2–5 than those of the major single component.*

### 3.3. Differential scanning calorimetry

Since transition temperatures from heating thermograms are reported at heat flow maxima (rather than at the onset of heat flow), they are always slightly higher than those from optical microscopy. When repeated scans were recorded to obtain information about the reversibility of Cr → LC transitions, samples were not heated to their clearing temperatures, to avoid decomposition.

CAQ cooled from the cholesteric phase crystallizes in a different, more disordered packing arrangement (Cr') than the one obtained through solvent recrystallization (Cr). On first heating, solvent-crystallized CAQ showed an endothermic Cr → LC transition at 166°C

( $\Delta H = 55 \text{ J g}^{-1}$ ). Cooling led to an exothermic LC → Cr' transition at 135°C ( $\Delta H = 15 \text{ J g}^{-1}$ ). During the second cycle, Cr' → LC was observed at 169.7°C ( $\Delta H = 25.9 \text{ J g}^{-1}$ ) while LC → Cr' remained virtually unchanged; all subsequent cycles reproduced the second one. The melt-derived Cr' phase persists for very long periods and may be thermodynamically favoured. After 10 months at room temperature, a sample initially in the Cr' phase had  $T_{Cr' \rightarrow LC}$  at 168.5°C ( $\Delta H = 26.1 \text{ J g}^{-1}$ ) and  $T_{LC \rightarrow Cr'}$  at 133.8°C ( $\Delta H = 17.03 \text{ J g}^{-1}$ ). Consecutively run CMAQ thermograms did not show appreciable differences.

DSC results from first heating scans were not reproducible (due to the aforementioned sample heterogeneities), but those from subsequent heating and cooling scans were. Averaged values of transition enthalpies and temperatures are reported in table 2. Both were virtually unchanged after solid samples that had been heated to the LC phase and cooled at least once were incubated for one or two weeks at room temperature in a dry atmosphere.

A slight increase in enthalpy and temperature of a lower temperature heating endotherm (see below) was found in incubated CAQ:CMAQ mixtures containing 10–80 wt % CAQ; thermograms recorded immediately thereafter were similar to those prior to incubation. For purposes of clarity, the various transitions are denoted by symbols (see figures 3 and 4):  $\Omega$  for the heating endotherm at 50–60°C;  $\beta_1$  for lower temperature heating exotherm;  $\beta_2$  for the higher temperature heating exotherm; Cr → LC for the heating endotherm generally observed at 150–180°C; LC → Cr and LC → Cr' for the cooling exotherms. None of these transitions results from the small amounts of molecular decomposition since 8:2, 5:5, and 2:8 CAQ:CMAQ mixtures that had been heated and cooled in DSC experiments were analysed by HPLC (detection at 258 nm, 99:1 hexane:ethyl acetate as eluant on a silica column) and found to contain the same percentages of the two components as before heating.

The phase diagram in figure 5 shows that the temperatures and enthalpies of the Cr → LC transition change in a regular fashion from neat CAQ to mixtures near the 5:5 composition. When 15–40 wt % of CMAQ was added to CAQ, the transition temperatures were lower than those of neat CAQ, but the enthalpies were higher, figure 5(a). The Cr → LC temperatures and enthalpies have local maxima near 20 and 30 wt % of CMAQ, respectively, and minima near 50 wt %; Cr → LC transitions were not detected in mixtures with 20–40 wt % CAQ, and became barely discernible in the 15 wt % mixture ( $\Delta H \sim 0.4 \text{ J g}^{-1}$ ). The phase assignments in figure 5(b) are based on theoretical models [23] and microscopic observations (*vide infra*).

Table 1. Transition temperatures and ranges (in parentheses) of the cholesteric phases measured by optical microscopy on first heating of CAQ:CMAQ mixtures.

CAQ:CMAQ/wt:wt	Temperature and (range)°C
10:0	159–228 (69)
9:1	164–268 (104)
8:2	158–267 (109)
7:3	162–267 (105)
6:4	152–257 (105)
5:5	155–251 (96)
4:6	149–242 (93)
3:7	149–235 (86)
2:8	159–231 (72)
15:85	165–230 (65)
1:9	165–222 (57)
0:10	173–190 (17)



Table 2. Temperatures and enthalpies of CAQ:CMAQ mixtures measured by DSC for various transition types.

CMAQ/wt %	$\Omega$		$\beta 1$		$\beta 2$		Cr $\rightarrow$ LC		LC $\rightarrow$ CR	
	$\Delta H/J g^{-1}$	$T/^\circ C$	$\Delta H/J g^{-1}$	$T/^\circ C$	$\Delta H/J g^{-1}$	$T/^\circ C$	$\Delta H/J g^{-1}$	$T/^\circ C$	$\Delta H/J g^{-1}$	$T/^\circ C$
0							25.9	169.7	15.4	135.3
5							27.9	169.4	20.2	133.7
10							24.3	163.1	16.1	113.9
15			7.1	139.1			29.6	164.7	14.6	116.1
20			14	127.9			38.5	166.5	14.1	100.1
30	3.9	64.1	13.7	88.2	16.6	122.7	33.0	167.0		
40	3.2	57.8	13.4	116.3	10.2	122.9	29.6	164.4		
50	1.5	55.5			9.7	138.7	9.6	159.9		
60	3.0	56.3					0			
70	2.2	55.1					0			
80	2.3	54.6					0			
85	2.3	54.0					0.4	175.8		
90	1.9	54.2			14.5	148	16.6	177.1		
100							66.9	181.8	44	123

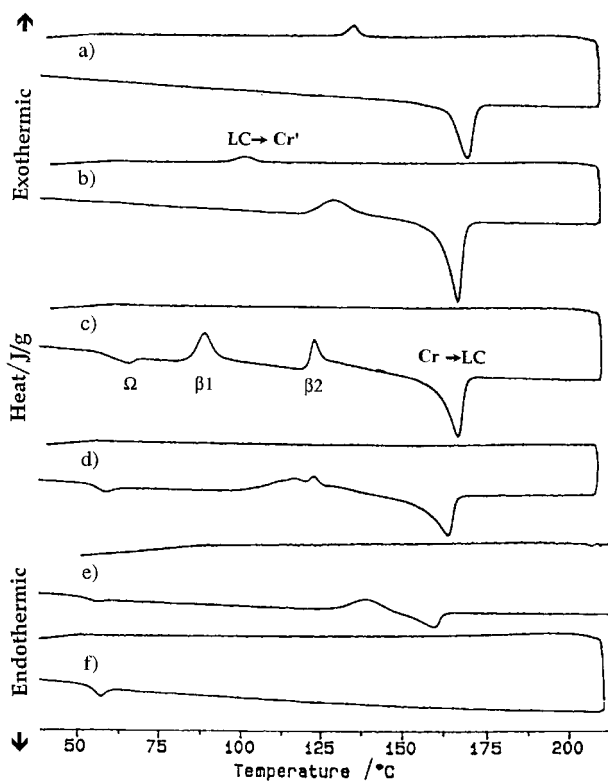


Figure 3. Second heating/cooling DSC thermograms of (a) 10:0, (b) 8:2, (c) 7:3, (d) 6:4, (e) 5:5, and (f) 4:6 CAQ:CMAQ mixtures.

On cooling, the enthalpy of LC  $\rightarrow$  Cr' decreased generally as the fraction of CMAQ increased until the transition was no longer detectable in 7:3 CAQ:CMAQ (figure 3) and the  $\Omega$  transition appeared (table 2). The temperature of  $\Omega$  varied by only *c.* 6° in mixtures with 0–60 wt % CAQ. At 50–70 wt % CAQ, the magnitude of the enthalpy of the  $\Omega$  endotherm was smaller than

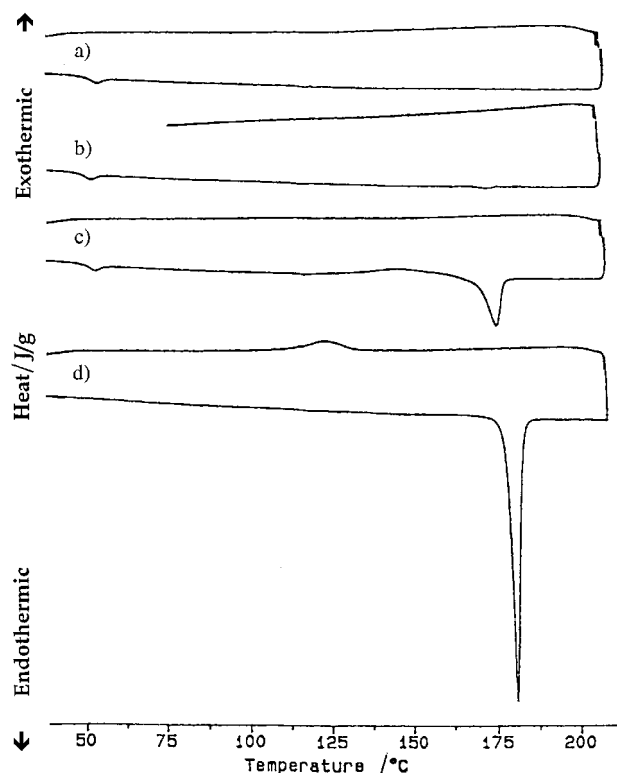


Figure 4. Second heating/cooling DSC thermograms of (a) 2:8, (b) 15:85, (c) 1:9, and (d) 0:10 CAQ:CMAQ mixtures.

that of the  $\beta 1$  and  $\beta 2$  exotherms observed at higher temperature; the absorbed energy was not released completely. The  $\Omega$  is the only transition that could be observed in the second heating cycle of mixtures with 20–40 wt % CAQ (figure 5); the negative slopes of the baselines in these thermograms (figures 3 and 4) are due to an instrumental artifact. When the 4:6 mixture was

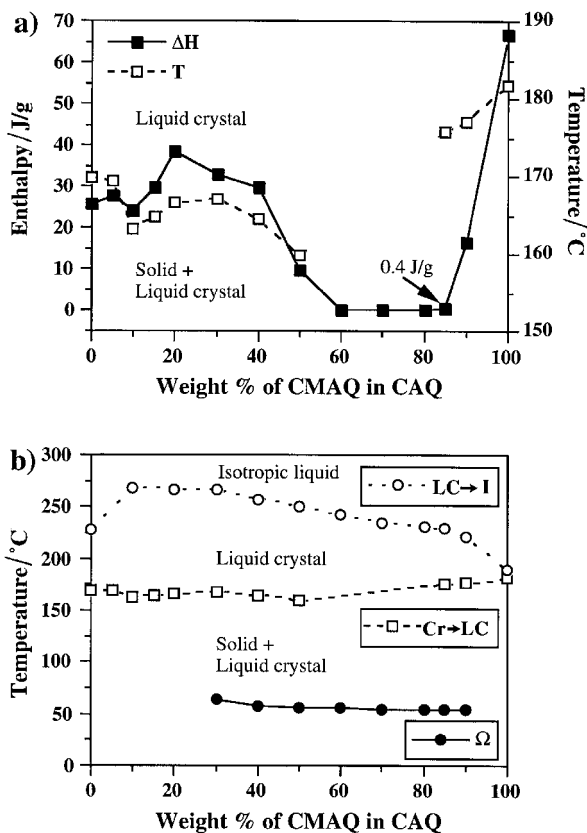


Figure 5. Phase diagrams for mixtures of CAQ and CMAQ. (a) Enthalpy ( $\blacksquare$ ) and temperature ( $\square$ ) of the Cr $\rightarrow$ LC transition versus wt% of CMAQ from DSC. (b) Temperatures of Cr $\rightarrow$ LC ( $\square$ ) and  $\Omega$  transitions ( $\bullet$ ) from DSC and clearing transitions ( $\circ$ ) from optical microscopy as a function of wt% of CMAQ. The lines are empirical connections only.

heated to and cooled from 80°C, the  $\Omega$  transition could be observed in subsequent heating thermograms.

At  $\leq 85$  wt% of CAQ,  $\beta_1$  was detected at 139.1°C ( $\Delta H = 7.1 \text{ J g}^{-1}$ );  $\beta_2$ , and  $\Omega$  were detected in samples with  $\leq 70$  wt% CAQ (figures 4 and 5 and table 2).  $\beta_1$  and  $\beta_2$  seem to coalesce in the 6:4 mixture while the 5:5 mixture showed only one transition, probably  $\beta_2$ . This assignment is based upon the observation that  $\beta_2$  occurs at a higher temperature than  $\beta_1$  in the 7:3 mixture. Except at low CMAQ content, the enthalpy change associated with  $\beta_2$  was not affected by composition, but the transition temperature decreased gradually (table 2). The temperatures of  $\beta_1$  and  $\beta_2$  do not follow similar trends.

### 3.4. X-ray diffraction

The molecular structure and packing of CAQ in the Cr phase (crystallized from toluene/1-butanol) were determined by single-crystal X-ray diffraction [24]. There are no clearly discernible  $\pi$ - $\pi$  interactions between

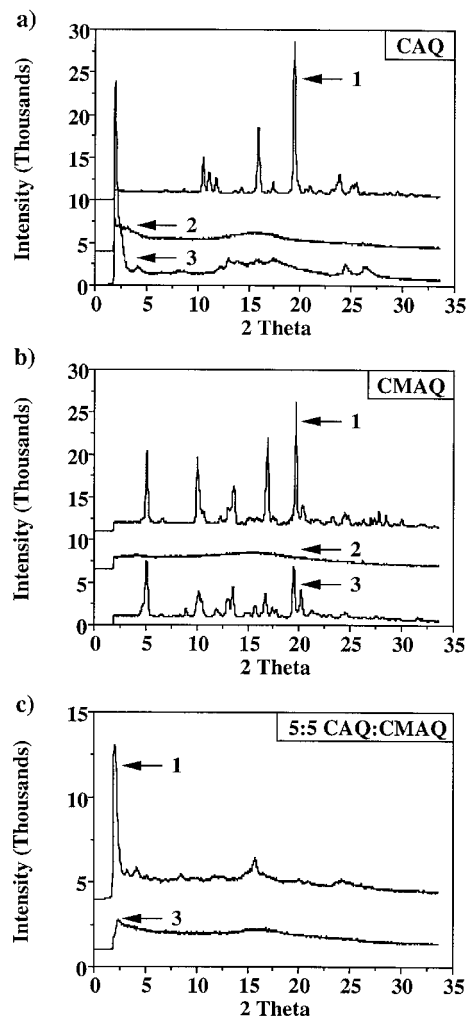


Figure 6. X-ray powder diffraction patterns of (a) CAQ, (b) CMAQ, and (c) 5:5 CAQ:CMAQ. Curve 1: small crystals of CAQ and CMAQ from ethyl acetate and 5:5 CAQ:CMAQ from evaporation of methylene chloride solution. Curve 2: mesophases at (a) 180°C and (b) 195°C. Curve 3: after cooling from the mesophases at (a) 70°C, (b) 113°C, and (c) 30°C. The curves have been offset vertically for clarity.

adjacent anthraquinonyl groups or important steric interactions between cholesteryl groups; all intermolecular distances are at least 3.9 Å.

Distinct differences are apparent between the powder diffraction patterns of the Cr and Cr' phases of CAQ, figure 6(a). Cr' is not a super cooled liquid crystalline phase. Its diffraction feature at  $2\theta = 2.5^\circ$  corresponds to a Bragg distance of 46 Å and indicates long-range order. Since the calculated molecular length of CAQ is  $c. 27$  Å and the length of the anthraquinonyl moiety is  $c. 9$  Å,‡

‡A molecular mechanics optimization was performed with the Hyperchem modeling software (by HyperCube) using the Polak-Ribiere conjugate gradient; rms gradient of 0.1 kcal/mol to a maximum of 1470 cycles.



46 Å may represent the thickness of a partially interdigitated layer with partially overlapping head-to-tail aromatic groups (based on electronic spectra [10, 11]) or to layers of non-interdigitated molecules whose long axes are tilted with respect to their lamellar planes. The arrangement may be like that of the cholesteric mesophase since a similar low-angle peak is observed in its diffraction pattern.

Powder X-ray diffraction patterns of the Cr and cooled-melt solid phases of CMAQ are very similar, figure 6(b). Relative intensity differences in the two patterns may be caused by partial orientation of microcrystallites that occur upon cooling from the mesophase. These data suggest that the structures of Cr and the solid from the cooled melt of CMAQ are the same.

The mesophases of CAQ and CMAQ have similar diffraction features, including a broad peak centred at  $c. 15^\circ$  (corresponding to an intermolecular spacing of  $c. 5 \text{ \AA}$ ) that is commonly observed in nematic and cholesteric phases. A low angle peak in the liquid crystalline phases, normally associated with a smectic or other layered phases, may be due to residual solid that remained as a result of a temperature gradient along the sample capillary. Optical micrographs do not support the presence of a smectic phase in neat CAQ or CMAQ and, if one were present, the Bragg distances associated with the low-angle diffractions would require either severe conformational bending or molecular tilting to retain a layered arrangement.

Powder patterns of the 8:2 solid before and after heating to the mesophase are very similar. Both include a small angle peak like that obtained from the Cr phases of CAQ. The similarity of the diffraction patterns from a 'solid' 5:5 mixture after cooling from the mesophase and from the liquid crystalline phases of CAQ and CMAQ is consistent with the former being a glassy (supercooled) mesophase and with the previously noted absence of a detectable DSC exotherm upon cooling, figure 6(c). The diffraction pattern of a 5:5 mixture from evaporation of a  $\text{CH}_2\text{Cl}_2$  solution also resembles that of an intimate mixture.

### 3.5. Calculation of eutectic compositions

Since some binary mesogenic mixtures are known to be eutectic [2, 23, 25], we explored the possibility that CAQ:CMAQ might also exhibit such behaviour. The composition of a eutectic mixture can be predicted by the Schröder–van Laar equations (2) and (3) if the components and their mixtures behave ideally, are completely miscible [23], and do not participate in strong intermolecular interactions. In these equations,  $\Delta H_{f1}$  and  $T_1$ , and  $\Delta H_{f2}$  and  $T_2$  are the heats and temperatures

of fusion of components 1 and 2, respectively, and  $T$  is the temperature of fusion for a system in which  $\chi_1$  is the mole fraction of component 1. Plotting the two equations for a binary system should result in two lines whose point of intersection (9:1 CAQ:CMAQ here) defines the composition of the eutectic mixture (figure 7) if the two components behave ideally. Since the temperatures of Cr  $\rightarrow$  LC transitions are plotted, the intersection point represents the equilibrium between crystal and liquid crystalline phases.

$$-\ln \chi_1 = (\Delta H_{f1}/R)(1/T - 1/T_1) \quad (2)$$

$$-\ln(1 - \chi_1) = (\Delta H_{f2}/R)(1/T - 1/T_2) \quad (3)$$

## 4. Discussion

CAQ and CMAQ are virtually isostructural except for the presence of two methyl groups on the 9,10-anthracenyl oxygen atoms in the latter. Optical micrographs demonstrate that neat CAQ and CMAQ form enantiotropic cholesteric liquid crystalline phases and their similar X-ray powder diffraction patterns indicate similar intermolecular separations. Nevertheless, the liquid crystalline temperature ranges differ by  $c. 50^\circ$ , due in large part to differences in  $\pi$ - $\pi$ , steric, and dipolar interactions. As molecular mobility increases (at higher temperatures), the additional disorder caused by motions of the CMAQ methoxy groups must contribute to its lower clearing temperature. Thus, the melting point of 9,10-anthraquinone (285–286°C [26]) is more than  $80^\circ$  higher than that of 9,10-dimethoxyanthracene (202°C [26]). By contrast, preferential  $\pi$ - $\pi$  stacking and a non-zero dipole moment [15, 16] of dimethoxyanthracenyl moieties may be responsible for CMAQ having the higher  $T_{\text{Cr} \rightarrow \text{LC}}$ .

$3\beta$ -Cholesteryl anthracene-2-carboxylate (CA-2) [19], which lacks the two methoxy groups of CMAQ but is

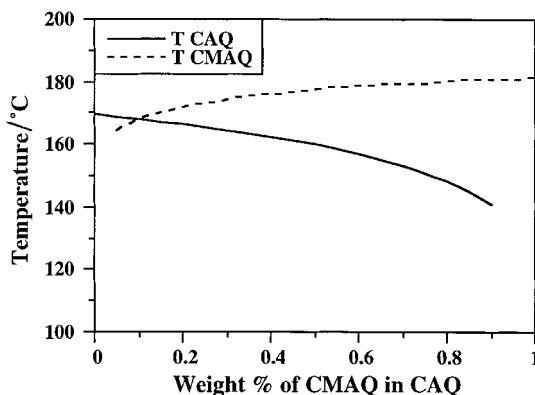
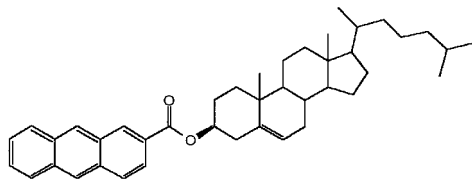


Figure 7. Schröder–van Laar plots of CAQ and CMAQ. See text for details.

similar in shape to CAQ, exhibits an enantiotropic cholesteric mesophase over only  $5^\circ$  (between 220 and  $225^\circ\text{C}$ ).



CA-2

The addition of only 10 wt % CMAQ to CAQ causes a  $40^\circ$  increase in the clearing temperature during the first heating cycle. We suspect that a CT complex like that detected at room temperature is the probable cause of the increase in the clearing temperature $\S$ . Its existence can be inferred from the orange colour of mixtures in the liquid crystalline phase.

Although the stoichiometries of the CT complexes have not been determined, there is significant circumstantial evidence for more than one. The strengths of the different possible CT interactions in the mesophase mixtures may be indicated by the clearing temperatures (table 1). Mixtures with 70–90 wt % CAQ have the same clearing temperatures; a gradual decrease of the clearing temperatures upon increasing the CMAQ content is consistent with the behaviour of other binary mixtures [2–5]. Since the clearing temperatures and enthalpies of Cr $\rightarrow$ LC transitions are higher and the mesophase ranges are larger in compositions near 8:2 than in the 5:5 mixture, if a CT complex with 2/1 CAQ/CMAQ stoichiometry is formed (we exclude 4/1 and 3/1 for steric reasons), it is stronger and induces greater stability in the mesophases than does a 1/1 complex (N.B. the 5:5 mixture). CT stabilization, as measured by the criteria above, is not ‘symmetric’ about the 5:5 composition. There is a more pronounced decrease in the clearing temperatures and a smaller increase in the mesophase range for compositions with  $>50$  wt % CMAQ than for those with  $<50$  wt %, figure 5(a) and table 1.

The LC $\rightarrow$ Cr’ exotherms from cooling melts with 5–20 wt % CMAQ occurred at progressively lower temperatures. The corresponding enthalpies are nearly constant and similar to those of neat CAQ (but lower than the enthalpy of its Cr $\rightarrow$ LC transition). The lack of a discernible LC $\rightarrow$ Cr’ transition in mixtures with  $>20$  wt % CMAQ indicates that nucleation leading to phase-separated crystalline material is hampered, but the onset of the  $\Omega$  transition suggests that a new phase

is formed. Since the  $\Omega$  transition temperature is virtually independent of CMAQ concentration, a eutectic mixture may be responsible [1, 2, 10, 11, 23, 25]. Although the melting temperature of eutectic domains should be constant, it can be altered if the domains coexist with molecules in a different form. Since small increases occur in enthalpy and temperature for  $\Omega$  in samples annealed for one week at room temperature, the eutectic content may increase with time.

We postulate that significant amounts of the eutectic are present in mixtures with 20–40 wt % CAQ, and that a combination of steric and CT interactions suppresses their nucleation;  $\Omega$  is the only transition observable by DSC. Our inability to detect  $\Omega$  by optical microscopy is consistent with the properties of other eutectics. The eutectic composition, estimated to be *c.* 3:7 CAQ:CMAQ by extrapolation of the plot of Cr $\rightarrow$ LC temperatures vs. composition [figure 5(a)], is far from the 9:1 composition predicted by the Schröder–van Laar plots in figure 7. As mentioned, the influence of CT interactions on the thermodynamics of mixing is not considered in equations (2) and (3) [23]; CAQ:CMAQ mixtures are not ‘ideal’. In addition, the point of intersection in figure 7 is not well defined due to the small slopes of the individual curves.

The *exothermic* transitions observed upon heating mixtures with  $\geq 50$  wt % CAQ can be explained by a model that includes eutectic formation and CT complexes with possibly 2/1, 1/1, and 1/2 stoichiometries. Clearly, other models can be invoked, but we prefer the one outlined below. In it, the heating exotherms from samples with 20–50 wt % CAQ are from crystallization of aggregates as molecules in the glassy cholesteric phase become more mobile. The smectic-like textures observed by optical microscopy on second heating of 8:2 and 7:3 mixtures may indicate a tendency toward crystallization similar to that of 6:4 and 5:5 mixtures. The two exotherms probably do not represent transitions from a eutectic phase because they occur at temperatures higher than those of  $\Omega$ ; when not at the eutectic composition, theory predicts a mixture of solid and liquid crystalline domains at such temperatures [23]. Since the optical textures are not like two coexisting phases, the solid particles must be very small and well dispersed throughout the LC component. Based on white and yellow crystals observed by optical microscopy when 6:4 and 5:5 mixtures were heated, we assign the two exotherms to crystallization of excess CAQ in liquid crystalline matrices formed by CT complexes and crystallization of CAQ and CMAQ from CT complexes with 2/1 or 1/1 CAQ/CMAQ stoichiometries.

Regardless of whether 2/1, 1/1 or 1/2 CT complexes are thermodynamically favoured, enthalpy values for

$\S$ Since our UV-Vis sample holder cannot maintain temperatures where the mesophase exists (near  $200^\circ\text{C}$ ), no attempt was made to detect a CT band in the mesophase.

Cr→LC transitions of *all* mixtures probably include contributions from a distribution of complexed and uncomplexed molecules; the major CT component in each sample may be dictated by mixture composition (i.e. statistical factors).

We suggest that when  $\geq 50$  wt % CAQ is present, supercooled eutectic mixtures are formed by mostly 2/1 and 1/1 CAQ/CMAQ complexes. Heating the mixtures above the eutectic temperature allows uncomplexed and complexed CAQ molecules to gain sufficient mobility to form mesogenic domains and/or crystallize. The variations in enthalpy content of the  $\beta_1$  and  $\beta_2$  transitions indicate clearly the presence of more than one species undergoing solidification and that further heating leads to their melting. Although only one sharp transition was detected from 7:3 and 6:4 CAQ:CMAQ mixtures by optical microscopy, the two *heating* exotherms observed by DSC provide evidence for the coexistence of more than one aggregation form. The observation of only one exotherm in the 5:5 mixture is consistent with (but does not demand) crystallization primarily of 1/1 complexes.

When  $> 50$  wt % CMAQ is present, the thermal properties seem to be influenced solely by the formation of eutectic mixtures (from which crystallization is hampered) and CT complexes that stabilize the mesophase less than complexes in mixtures containing predominantly CAQ. The exotherm observed on heating 1:9 CAQ:CMAQ is probably from crystallization of complexed CAQ in a liquid crystalline matrix of CMAQ.

### 5. Summary

Although charge-transfer interactions have been exploited to induce or stabilize several thermotropic columnar discotic [5, 6], smectic A [8], and lyotropic nematic mesophases [9], no examples seem to have been reported for thermotropic cholesteric phases [27]. Here, we have demonstrated that charge-transfer interactions between mesomorphic molecules of very similar structure, CAQ and CMAQ, have a profound influence on the nature of the cholesteric and solid phases of their mixtures. The interactions extend the cholesteric mesophase temperature range, and lead to the formation of eutectics and CT complexes. Although attributions to some of the transitions detected by DSC are inferential, the data clearly demonstrate that a wide variety of molecular organizations is obtained.

We expect that judicious design of the structural and electronic properties of other cholesteric molecules will allow the mesophases of their charge-transfer stabilized mixtures to be temperature and pitch 'tuned' in ways that differ from conventional methods involving hydrogen-bonding or dipolar interactions.

We are extremely grateful to Prof. Tim Swager and Mr Bing Xu for use of their diffractometer and for their help in collecting the data and to Dr Quanlong Pu at the National Institutes of Health, Bethesda, Maryland, for the mass spectra. The National Science Foundation is thanked for its financial support.

### References

- [1] SHEIKH-ALI, B. M., and WEISS, R. G., 1995, *Liq. Cryst.*, **17**, 605.
- [2] DAVE, J. S., and DEWAR, M. J. S., 1955, *J. chem. Soc.*, 4305.
- [3] WEISS, R. G., 1998, *Mechanical and Thermophysical Properties of Polymeric Liquid Crystals*, edited by W. Brostow (London: Chapman & Hall), Chap. 1.
- [4] GRAY, G. W., 1962, *Molecular Structure and the Properties of Liquid Crystals* (New York: Academic Press).
- [5] See for instance (a) SAEVA, F. D., REYNOLDS, G. A., and KASZCZUK, L., 1982, *J. Am. chem. Soc.*, **104**, 3524; (b) PRAEFCKE, K., and SINGER, D., 1994, *Mol. Mat.*, **3**, 265.
- [6] MÖLLER, M., WENDORFF, J. H., WERTH, M., SPIESS, H. W., BENGIS, H., KARTHAUS, O., and RINGSDORFF, H., 1994, *Liq. Cryst.*, **17**, 381.
- [7] KOSAKA, Y., and URYU, T., 1994, *Macromolecules*, **27**, 6286.
- [8] FLETCHER, I. D., GUILLON, D., HEINRICH, B., OMENAT, A., and SERRANO, J. L., 1997, *Liq. Cryst.*, **23**, 51.
- [9] USOLTSEVA, N., PRAEFCKE, K., SINGER, D., and GUNDOGAN, B., 1994, *Liq. Cryst.*, **16**, 617.
- [10] OSTUNI, E., 1995, MS thesis, Georgetown University, Washington, DC, USA.
- [11] OSTUNI, E., and WEISS, R. G., 1995, 29th ACS Middle Atlantic Regional Meeting, Washington, DC, USA, abstract No. 238.
- [12] HEINIS, T., CHOWDHURY, S., SCOTT, S. L., and KEBARLE, P., 1988, *J. Am. chem. Soc.*, **110**, 400.
- [13] MIELERT, A., BRAIG, C., SAUER, J., MARTELLI, J., and SUSTMANN, R., 1980, *Liebigs Ann. Chem.*, **6**, 954.
- [14] MEREDITH, C. C., WESTLAND, L., and WRIGHT, C. F., 1957, *J. Am. chem. Soc.*, **79**, 2385.
- [15] LE FEVRE, R. J. W., SUNDARAM, A., and SUNDARAM, K. M. S., 1963, *J. chem. Soc.*, 4447.
- [16] EVERARD, K. B., and SUTTON, L. E., 1951, *J. chem. Soc.*, **16**, 21.
- [17] DEMUS, D., and RICHTER, L., 1978, *Textures of Liquid Crystals* (New York: Verlag Chemie).
- [18] MEEK, J. S., MONROE, P. A., and BOUBOLIS, C. J., 1963, *J. org. Chem.*, **28**, 2572.
- [19] LIN, Y.-C., KACHAR, B., and WEISS, R. G., 1989, *J. Amer. chem. Soc.*, **111**, 5542.
- [20] KRELSKY, S., 1957, *Acta Chem. Scand.*, **11**, 913.
- [21] TERECH, P., OSTUNI, E., and WEISS, R. G., 1996, *J. phys. Chem.*, **100**, 3759.
- [22] GIBSON, H. W., 1979, in *Liquid Crystals: The Fourth State of Matter*, edited by F. D. Saeva (New York: Marcel Dekker).

- [23] HSU, E. C. H., and JOHNSON, J. F., 1973, *Mol. Cryst. liq. Cryst.*, **27**, 95.
- [24] OSTUNI, E., KAMARAS, P., and WEISS, R. G., 1996, *Angew. Chem. intl. Ed. Engl.*, **35**, 1324.
- [25] VILALTA, P. M., HAMMOND, G. S., and WEISS, R. G., 1993, *Langmuir*, **9**, 1910.
- [26] RIGAUDY, J., and SPARFEL, D., 1972, *Bull. Soc. Chem. Fr.*, 3441.
- [27] WILLIAMS, V. E., and LEMIEUX, R. P., 1996, *Chem. Commun.*, 2259. CT has been discounted in favour of electrostatic repulsion and polarizability interactions leading to  $\pi$ -stacking as an explanation for the induction of cholesteric (i.e., twisted nematic) phases by addition of dibenzoxepins to 4-cyano-4'-pentylbiphenyl or 4-cyano-4'-pentyloxybiphenyl.